Title

Ex Vivo Analysis of Tryptophan Metabolism Using ^{19}F NMR.

Journal

ACS chemical biology, 14(9)

ISSN

1554-8929

Authors

Tombari, Robert J
Saunders, Carla M
Wu, Chun-Yi
et al.

Publication Date

2019-09-01

DOI

10.1021/acschembio.9b00548

Peer reviewed

HHS Public Access

Author manuscript

ACS Chem Biol. Author manuscript; available in PMC 2020 September 20.

Published in final edited form as:

ACS Chem Biol. 2019 September 20; 14(9): 1866–1873. doi:10.1021/acschembio.9b00548.

Ex Vivo Analysis of Tryptophan Metabolism Using ^{19}F NMR

Robert J. Tombari[1], **Carla M. Saunders**[1], **Chun-Yi Wu**[2], **Lee E. Dunlap**[1], **Dean J. Tantillo**[1], **David E. Olson**[1,3,4,*]

[1]Department of Chemistry, University of California, Davis, Davis, CA 95616, USA

[2]Bioanalysis and Pharmacokinetics Core Facility, University of California, Davis, Sacramento, CA 95817, USA

[3]Department of Biochemistry & Molecular Medicine, School of Medicine, University of California, Davis, Sacramento, CA 95817, USA

[4]Center for Neuroscience, University of California, Davis, Davis, CA 95616, USA

Abstract

Tryptophan—an essential amino acid—is metabolized into a variety of small molecules capable of impacting human physiology, and aberrant tryptophan metabolism has been linked to a number of diseases. There are three principal routes by which tryptophan is degraded, and thus, methods for measuring metabolic flux through these pathways can be used to understand the factors that perturb tryptophan metabolism and potentially to measure disease biomarkers. Here, we describe a method utilizing 6-fluorotryptophan as a probe for detecting tryptophan metabolites in ex vivo tissue samples via ^{19}F nuclear magnetic resonance. As a proof of concept, we demonstrate that 6-fluorotryptophan can be used to measure changes in tryptophan metabolism resulting from antibiotic-induced changes in gut microbiota composition. Taken together, we describe a general strategy for monitoring amino acid metabolism using ^{19}F nuclear magnetic resonance that is operationally simple and does not require chromatographic separation of metabolites.

Graphical Abstract

*Corresponding Author: deolson@ucdavis.edu.

Author Contributions

R.J.T. performed the NMR experiments. C.M.S. and D.J.T. performed and analyzed results from ^{19}F chemical shift calculations. C.-Y.W. performed LC-MS experiments. L.E.D. synthesized several 19F metabolites to be used as NMR standards. D.E.O. conceived the project and supervised experiments. D.E.O. and R.J.T. wrote the manuscript with input from all authors.

Supporting Information

Supporting Information Available: This material is available free of charge *via* the Internet.

Figure S1, Figure S2, Figure S3, Table S1, experimental procedures for the synthesis of fluorinated metabolites, and additional computational details

The authors declare no competing financial interest.

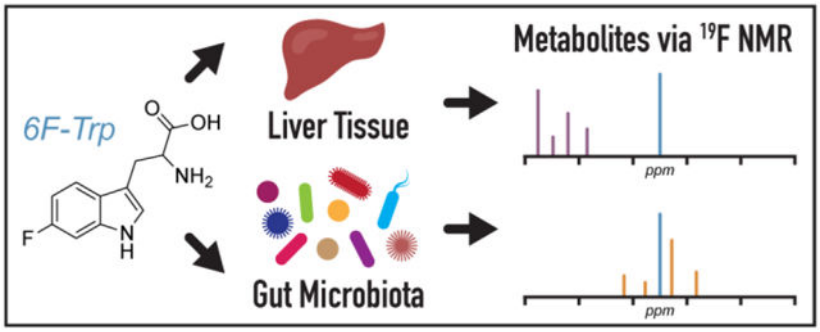

Keywords

Tryptophan; Metabolism; Fluorine; NMR; Microbiome

Tryptophan metabolism proceeds down three distinct pathways towards, 1) kynurenine-, 2) serotonin-, and 3) indole-related metabolites (Figure 1A). Changes in these metabolic fluxes have been associated with both normal aging[1] as well as a variety of pathological states[2] such as autism spectrum disorder,[3] depression,[4] Alzheimer's disease,[5] and autoimmune diseases,[6] among many others. In model organisms, manipulation of tryptophan metabolism has been shown to have profound effects. For example, inhibition of the kynurenine pathway prolongs the lifespan of *C. elegans*[7] and reduces neurodegeneration in *Drosophila* models of Alzheimer's and Parkinson's disease.[8] Methods capable of monitoring tryptophan metabolism are not only critical for elucidating basic biology, they also have the potential to identify biomarkers of disease.

Currently, most methods to measure tryptophan metabolism rely on liquid chromatography coupled to mass spectrometry (LC-MS).[9,10,11,12,13,14] These methods offer several advantages, including excellent sensitivity and high confidence regarding the identities of measured analytes. However, they require the generation of calibration curves, and often it can be challenging to develop chromatographic methods capable of separating the approximately 30 common tryptophan metabolites so that they can be measured simultaneously. Recently, Zhang and co-workers reported a method using ultra-performance liquid chromatography-selected reaction monitoring-mass spectrometry (UPLC-SRM-MS) that enabled the quantification of 31 tryptophan metabolites in various tissues.[15] While quite impressive, it is unclear how easily other laboratories could adopt this methodology given the equipment and expertise necessary to do so.

As an alternative to LC-MS, we have been investigating the potential for using nuclear magnetic resonance (NMR) spectroscopy to measure tryptophan metabolism. An NMR-based method would obviate the need for chromatographic purification—assuming that the metabolites all possess distinct, non-overlapping chemical shifts—and it would enable quantification simply by peak integration. Furthermore, it would have the potential to measure metabolic changes in vivo. In fact, in vivo magnetic resonance spectroscopy (MRS) is an ideal platform for measuring metabolites in specific organs, such as the brain, as it can non-invasively detect multiple compounds simultaneously in animals, including humans.[16] It

has been used previously to track the biodistribution of drugs as well as to determine metabolic fluxes.[17,18] While ^{1}H MRS has been used extensively in medical research, this method suffers from high background and a narrow chemical shift range, which makes it difficult to identify distinct compounds. Therefore, researchers have resorted to labeling precursors of interest with stable MRS-active isotopes such as ^{13}C. However, the limited sensitivity of the ^{13}C signal (1.6% of the ^{1}H signal) can hinder certain investigations. Furthermore, at 1.1% natural abundance, the ^{13}C contained within endogenous proteins and lipids still produces interfering background noise capable of masking signals from metabolism of the ^{13}C-labeled probe. To overcome these issues, researchers have explored various hyperpolarization techniques,[19] but the T_1 relaxation of ^{13}C is on the order of seconds to minutes making this technique unsuitable for measuring amino acid metabolism —a process that can take several hours.[20]

For these reasons, we have decided to pursue ^{19}F-labeled probes. The only natural isotope of fluorine is ^{19}F (100% abundance), and the sensitivity of ^{19}F NMR is 94% that of ^{1}H NMR.[21] Moreover, the elemental abundance of ^{19}F in the body is quite low (<0.01%), with most ^{19}F existing within solid teeth or bone structures resulting in a very short T_2 relaxation. Therefore, endogenous molecules containing ^{19}F will interfere minimally with the measurements of probe metabolites. Furthermore, ^{19}F NMR has the added bonus of providing a large chemical shift range, improving the odds that metabolite peaks will not have overlapping chemical shifts.

While ^{19}F-labeled probes offer many distinct advantages over analogous ^{13}C-labeled compounds for NMR applications, they suffer from one major drawback, namely, that they are unnatural versions of the molecule they are designed to study. Fluorine is often regarded as an ideal bioisostere for hydrogen due to its small size (Van Der Waals radii of 1.2 and 1.47 Å for H and F, respectively);[22,23] however, it can exert a strong electronic influence due to its large electronegativity.[24] Therefore, an appropriate fluorinated probe would have to be carefully designed. We reasoned that fluorination of tryptophan's indole would be unlikely to affect either the transport of the probe across membranes by the large neutral amino acid transporter (LAT1) or the decarboxylation by aromatic amino acid decarboxylase (AADC) as this transporter and enzyme, respectively, have demonstrated tolerance for variation at the amino acid side chain.[25,26] However, choosing which position of the indole to fluorinate was not as straightforward.

Tryptophan is enzymatically oxidized at the 5-position to produce 5-hydroxytryptophan and at the 2- and 3-positions to produce N-formylkynurenine, leading to metabolites of the serotonin and kynurenine pathways, respectively (Figure 1A). In principle, fluorination of the 6- and 7-positions should enable normal metabolic processing of the probe; however, Wiseman and co-workers reported that tryptophan 2,3-dioxygenase oxidizes 7-F-tryptophan at a reduced rate in vitro as compared to tryptophan.[27] Fortunately, 6-F-tryptophan has been reported to exhibit rates of oxidation at the 5- and 2,3-positions comparable to or greater than tryptophan itself.[15,28] Thus, we chose to investigate 6-F-tryptophan (6-F-Trp) for our studies. Previously, 6-F-Trp had been used to study protein unfolding by NMR[29] as well as serotonin turnover in the brains of rats.[30]

To ensure that 6-F-Trp was metabolized in a similar fashion as the parent compound, we first incubated mouse liver homogenates at 37 °C with either racemic tryptophan or racemic 6-F-Trp and analyzed the samples using LC-MS. After 2 h, we observed the expected peaks corresponding to kynurenine and 4-F-kynurenine, respectively, verifying that the probe can be metabolized in a similar manner as the natural amino acid (Figure S1).

Next, we incubated ex vivo samples with the racemic 6-F-Trp and observed the formation of new metabolite peaks as a function of time via ^{19}F NMR (Figure 2A and Table S1). We used 3.75 mM trifluoroacetic acid (TFA) as an internal standard[31] and obtained spectra with adequate signal to noise ratios after only 8 mins of acquisition time. As reported by Zhang and co-workers,[15] tryptophan metabolism appeared to be highly dependent on the tissue or sample being studied. In our case, samples from rat liver and feces produced entirely different metabolic profiles (Figure 2A and B). Moreover, the method of preparing the tissue impacted which metabolites were observed. Grinding the tissue with a mortar and pestle after cryogenic freezing (i.e. “cryoground” tissue) is a technique often used to extract enzymes.[32] However, we found that the supernatant from cryoground tissue produced a fewer number of metabolites than that from fresh tissue, though the major metabolites were the same (Figure 2B). We hypothesize that fresh samples contain higher concentrations of active metabolic enzymes resulting in a greater number of metabolites reaching concentrations exceeding our limit of detection.

Under our experimental conditions, it is possible that protein binding could impact the observed chemical shifts and/or T_2 relaxation of various metabolites. As a control experiment, we dissolved 6-F-Trp or 3-F-aniline in our incubation buffer containing increasing concentrations (up to 100 mg/mL) of bovine serum albumin (BSA; Figure S2). Even at high protein concentrations, the observed chemical shift never varied by more than 0.02 ppm. In the case of 3-F-aniline, the apparent analyte concentration (using TFA as an internal standard) increased slightly as protein concentration increased while the opposite was true for 6-F-Trp (Figure S2). In both cases, higher protein concentrations resulted in reduced signal to noise ratio. When samples contain large amounts of protein and low signal to noise ratios are observed, we recommend performing a protein precipitation step to break up any potential interactions between the metabolites and biomacromolecules.

We chose to use racemic 6-F-Trp as a probe for two reasons. First, this compound is commercially available and significantly less expensive than *S*-6-F-Trp. Second, we reasoned that the unnatural *R*-enantiomer was unlikely to be metabolized as efficiently as the natural *S*-enantiomer, and thus, residual *R*-6-F-Trp could be used as a chemical shift landmark. For most samples (e.g., cryoground liver, cryoground feces, fresh feces), this appeared to be true as >50% of the total fluorine signal could be attributed to the 6-F-Trp probe (Figure 2C). However, after incubation in supernatant obtained from fresh liver, 6-F-Trp only accounted for ~40% of the total fluorine signal in the NMR (Figure 2C). This indicates that at least 10% of *R*-6-F-Trp was metabolized by the fresh liver preparation—likely due to either the presence of more promiscuous enzymes or racemization followed by metabolism of the *S*-enantiomer.

As the majority of the compounds produced by the metabolism of 6-F-Trp are not commercially available or readily synthesized, we turned to computation to assist with prediction of their ^{19}F chemical shifts. We calculated the chemical shifts for a large number of potential metabolites using density functional theory (DFT; Table 1; see Computational Methods and SI for details). To validate our method, we compared the calculated and experimental chemical shifts for six compounds (four metabolites and two controls) and found the deviations to be < 1.6 ppm. While we cannot easily distinguish between closely related structures (e.g., 6-F-Trp and 6-fluoro-tryptamine), we can differentiate compounds originating from the three major tryptophan metabolic pathways owing to their large structural differences (and hence chemical shift differences). For example, the ^{19}F NMR chemical shifts of indole-related metabolites are similar to that of the 6-F-Trp probe as the electronics of the aromatic ring have not been drastically altered. However oxidative cleavage of the indole or oxidation of the 5-position place the fluorine in very different chemical environments. As an approximation, kynurenine-, indole-, and serotonin-related metabolites have ^{19}F NMR chemical shifts in the ranges of −90 to −115, −115 to −130, and −130 to −150 ppm, respectively (Figure 1B). The only exceptions appear to be hydroxylated kynurenine metabolites such as 4-F-3-hydroxykynurenine, 6-F-3-hydroxyanthranilic acid, and 6-F-xanthurenic acid. The chemical shifts of these compounds more closely resemble those of metabolites from the serotonin pathway, as they all possess a hydroxyl group *ortho* to the fluorine. Using this method, we can clearly see that liver samples metabolize tryptophan via the kynurenine pathway while fecal samples favor indole-related metabolites (Figure 2B). To reliably differentiate between metabolites with closely related structures, we recommend that spiking experiments be performed using authentic standards.

Next, we were interested in using 6-F-Trp to measure tryptophan metabolism by gut microbiota, as these bacteria are well known to impact brain health.[33,34,35,36] Approximately 4–6% of ingested Trp is metabolized by bacteria in the gut,[37] and tryptophan metabolites are particularly important players in the gut-brain axis.[38,39] We collected fecal samples from male and female Sprague Dawley rats before antibiotic administration, immediately after 7 days of treatment, and approximately two weeks after the cessation of treatment (Figure 3A). Approximately 30% of the fluorinated probe was metabolized by fecal samples obtained prior to antibiotic administration (Figure 3B and C) and no major differences between sexes were observed. Following a week of antibiotic treatment, almost none of the fluorinated probe was metabolized by fecal samples, emphasizing the critical role that bacteria play in this process (Figure 3B and C). Following a recovery period of approximately two weeks without antibiotics, tryptophan metabolism began to recover; however, probe consumption never reached that of pre-antibiotic levels (Figure 3C). Moreover, the balance of tryptophan metabolites did not return to normal following cessation of antibiotic treatment (Figure 3D and Figure S3) indicating a change in the composition of the gut microbiome. Antiobiotics are known to promote gut microbiome dysbiosis,[40] and it appears that this disruption can be measured at the level of tryptophan metabolism.

In conclusion, we have developed a fluorinated analog of tryptophan enabling the study of tryptophan metabolism using ^{19}F NMR without the need for chromatography. We used this probe to demonstrate that tryptophan metabolism in the liver and gut proceeds down

distinction metabolic pathways, and that gut microbiome metabolism is disrupted by antibiotic treatment. The table of calculated chemical shifts that we provide should serve as a resource for those interested in using 6-F-Trp to study tryptophan metabolism in a variety of contexts or to identify biomarkers of disease. With the advent of benchtop NMR, we anticipate that probes like 6-F-Trp will be used for a wide range of applications, and we hope that the methods outlined here will serve as a general strategy for those interested in studying amino acid metabolism using ^{19}F NMR. Future work will determine if such probes are suitable for measuring tissue-specific metabolism using in vivo MRS.

Methods

Animals.

Sprague Dawley rats were obtained from Charles River Laboratories (Wilmington, MA, USA). Liver tissue was taken following CO_2 euthanasia. To collect fecal samples, animals were placed in a clean cage until they defecated. All experimental procedures involving animals were approved by the University of California, Davis Institutional Animal Care and Use Committee (IACUC) and adhered to principles described in the National Institutes of Health Guide for the Care and Use of Laboratory Animals. The University of California, Davis is accredited by the Association for Assessment and Accreditation of Laboratory Animal Care, International (AAALAC), and has an Animal Welfare Assurance number (#A3433–01) on file with the Office of Laboratory Animal Welfare (OLAW).

Chemistry (General).

All reagents were obtained commercially unless otherwise noted. Solvents were purified by passage under 12 psi N_2 through activated alumina columns. Chromatography was performed using Fisher Chemical™ Silica Gel Sorbent (230–400 Mesh, Grade 60). Compounds purified by chromatography were typically applied to the adsorbent bed using the indicated solvent conditions with a minimum amount of added dichloromethane as needed for solubility. Thin layer chromatography (TLC) was performed on Merck silica gel 60 F254 plates (250 μm). Visualization of the developed chromatogram was accomplished by fluorescence quenching or by staining with butanolic ninhydrin, aqueous potassium permanganate, ethanolic vanillin, or aqueous ceric ammonium molybdate (CAM).

Nuclear magnetic resonance (NMR) spectra were acquired on either a Bruker 400 operating at 400 and 100 MHz or a Varian-600 operating at 600 and 150 MHz for ^{1}H and ^{13}C, respectively, and are referenced internally according to residual solvent signals. Data for ^{1}H NMR are recorded as follows: chemical shift (δ, ppm), multiplicity (s, singlet; br s, broad singlet; d, doublet; t, triplet; q, quartet; quint, quintet; sext, sextet; m, multiplet), integration, and coupling constant (Hz). Data for ^{13}C NMR are reported in terms of chemical shift (δ, ppm).

Chemistry (Synthetic Details).

The specific procedures used to synthesize the compounds reported in this manuscript are detailed in the Supporting Information along with characterization data.

Computational Experiments.

Geometry optimizations were run using B3LYP/6–31+G(d,p) in the gas phase using *Gaussian09* and resulting structures were confirmed as minima using frequency calculations.[41,42,43,44,45,46] These structures were subjected to NMR (GIAO)[47] calculations at the B3LYP/6–311+G(2d,p) level using the SMD implicit solvent model for water.[48] For each metabolite with conformational flexibility, conformational searches were run with *Spartan10*, and then optimized in *Gaussian09* with B3LYP/6–31+G(d,p) in the gas phase.[41,49,50] Conformers within 3 kcal/mol of the lowest energy conformer were included in the NMR calculations, with their contributions weighted with a Boltzmann distribution based on their relative free energies. A linear scaling approach was used as described by Tantillo and co-workers (see SI for details).[51]

Ex Vivo Analysis of Metabolism from Fresh Samples.

For these experiments, samples were collected from adult female Sprague Dawley rats. Samples were placed in falcon tubes with a buffered solution (pH = 7.2) of PBS (0.1 M) with EDTA (2 mM), such that the liver and fecal samples reached concentrations of 2.5 and 0.1 g/mL, respectively. The samples were homogenized by hand using two opposite facing scalpels in a blending motion for five minutes. Homogenized tissue was then pelleted by centrifugation for 3 minutes at 3,200 x g at 21 °C. The supernatant was then added to a fresh falcon tube and incubated at 37 °C with 1 mg mL^{-1} of *R,S*-6-F-Trp. Samples were inverted daily to facilitate mixing and dissolution of probe. At the indicated time point, 0.54 mL of each sample was placed in an NMR tube and spiked with 0.06 mL of a 3.75 mM TFA solution in D_2O that had been adjusted to pH ≈ 6.0 using K_2CO_3. The resulting pH of the sample remained pH 7.2 after addition of the TFA standard. Next, ^{19}F NMR spectra were collected. Metabolism of 6-F-Trp in liver and fecal samples was monitored at 0 h, 24 h, 48 h, and 120 h.

Ex Vivo Analysis of Metabolism from Frozen Samples.

Samples were flash frozen with liquid nitrogen and stored at −80 °C for up to 4 months before homogenization via a mortar and pestle.[32] A buffered solution (pH = 7.2) of PBS (0.1 M) with EDTA (2 mM), was added to the ground samples such that the liver and fecal samples reached concentrations of 2.5 and 0.1 g/mL, respectively. The mixtures were sonicated six times at room temperature for 20 s, with 1 min intervals of chilling at 0 °C between rounds of sonication. Samples were then pelleted by centrifugation for 3 minutes at 3,200 x g at 4 °C. The supernatant was then added to a fresh falcon tube and incubated at 37 °C with 1 mg mL^{-1} of *R,S*-6-F-Trp. Samples were inverted daily to facilitate mixing and dissolution of the probe. At the indicated time point, 0.54 mL of each sample was placed in an NMR tube and spiked with 0.06 mL of a 3.75 mM TFA solution in D_2O containing that had been adjusted to pH ≈ 6.0 using K_2CO_3. The resulting pH of the sample remained pH 7.2 after addition of the TFA standard. Next, ^{19}F NMR spectra were collected. Metabolism of 6-F-Trp in liver and fecal samples was monitored at 0 h, 24 h, 48 h, and 120 h.

^{19}F NMR Analysis.

The metabolism of the probe was monitored using ^{19}F NMR with proton decoupling. TFA was used as an internal standard and referenced to −75.25 ppm.31 Peak areas were integrated over the same ppm region between experiments. Signals were deemed peaks if the integration area was greater than 0.03 when the TFA internal standard was set to 1.00.

Antibiotic Experiments.

Baseline fecal samples were collected on day 0 from 4 male and 4 female Sprague Dawley rats (P56) and processed according to the fresh extraction protocol described above. After collecting the baseline sample, the rats were administered a solution of USP grade penicillin G sodium salt (2 mg mL^{-1}) and USP grade streptomycin sulfate (4 mg mL^{-1}) in their drinking water. Water was changed every three days. Water consumption increased during the period of antibiotic administration. On day 7, fecal samples were collected and handled according to the fresh extraction protocol described above. The animals were then given pure water without antibiotics for the next 13 days. On day 20, fecal samples were collected and handled according to the fresh extraction protocol described above.

Supplementary Material

Refer to Web version on PubMed Central for supplementary material.

ACKNOWLEDGMENTS

We thank T. Jue, M. Augustine, A. Yu, M. Gareau, M. Pusceddu, and D. Murray for helpful discussions.

Funding

This work was supported by funds from the UC Davis Department of Chemistry (D.E.O.), Department of Biochemistry & Molecular Medicine (D.E.O.), a UC Davis New Research Initiatives and Collaborative Interdisciplinary Research Grant (D.E.O), and an NIH T32 Fellowship (T32GM113770 to R.J.T.). We also thank the NSF XSEDE program (CHE030089) for computational support.

REFERENCES

1. van der Goot AT and Nollen EA (2013) Tryptophan metabolism: entering the field of aging and age-related pathologies. Trends Mol. Med 19, 336–344. [PubMed: 23562344]
2. Chen Y and Guillemin GJ (2009) Kynurenine pathway metabolites in humans: disease and healthy states. Int. J. Tryptophan Res 2, 1–19. [PubMed: 22084578]
3. Boccuto L, Chen C-F, Pittman AR, Skinner CD, McCartney HJ, Jones K, Bochner BR, Stevenson RE, and Schwartz CE (2013) Decreased tryptophan metabolism in patients with autism spectrum disorders. Mol. Autism 4, 1–10. [PubMed: 23311570]
4. Oxenkurg GF (2010) Tryptophan-kynurenine metabolism as a common mediator of genetic and environmental impacts in major depressive disorder: the serotonin hypothesis revisited 40 years later. Isr. J. Psychiatry Relat. Sci 47, 56–63. [PubMed: 20686200]
5. Guillemin GJ and Brew BJ (2002) Implications of the kynurenine pathway and quinolinic acid in Alzheimer's disease. Redox Rep. 7, 199–206. [PubMed: 12396664]
6. Opitz CA, Wick W, Steinman L, and Platten M (2007) Tryptophan degradation in autoimmune diseases. Cell. Mol. Life Sci 64, 2542–2563. [PubMed: 17611712]
7. van der Goot AT, Zhu W, Vazquez-Manrique RP, Seinstra RI, Dettmer K, Michels H, Farina F, Krijnen J, Melki R, Buijsman RC, Ruiz Silva M, Thijssen KL, Kema IP, Neri C, Oefner PJ, and Nollen EA (2012) Delaying aging and the aging-associated decline in protein homeostasis by

inhibition of tryptophan degradation. Proc. Natl. Acad. Sci. U. S. A 109, 14912–14917. [PubMed: 22927396]

8. Breda C, Sathyasaikumar KV, Sograte Idrissi S, Notarangelo FM, Estranero JG, Moore GG, Green EW, Kyriacou CP, Schwarcz R, and Giorgini F (2016) Tryptophan-2,3-dioxygenase (TDO) inhibition ameliorates neurodegeneration by modulation of kynurenine pathway metabolites. Proc. Natl. Acad. Sci. U. S. A 113, 5435–5440. [PubMed: 27114543]
9. de Jong WH, Smit R, Bakker SJ, de Vries EG, and Kema IP, (2009) Plasma tryptophan, kynurenine and 3-hydroxykynurenine measurement using automated on-line solid-phase extraction HPLC-tandem mass spectrometry. J. Chromatogr. B Analyt. Technol. Biomed. Life Sci 887, 603–609.
10. Zhu W, Stevens AP, Dettmer K, Gottfried E, Hoves S, Kreutz M, Holler E, Canelas AB, Kema I, and Oefner PJ (2011) Quantitative profiling of tryptophan metabolites in serum, urine, and cell culture supernatants by liquid chromatography-tandem mass spectrometry. Anal. Bioanal. Chem 401, 3249–3261. [PubMed: 21983980]
11. Moller M, Du Preez JL, and Harvey BH (2012) Development and validation of a single analytical method for the determination of tryptophan, and its kynurenine metabolites in rat plasma. J. Chromatogr. B Analyt. Technol. Biomed. Life Sci 898, 121–129.
12. Huang Y, Louie A, Yang Q, Massenkoff N, Xu C, Hunt PW, and Gee W (2013) A simple LC-MS/MS method for determination of kynurenine and tryptophan concentrations in human plasma from HIV-infected patients. Bioanalysis 5, 1397–1407. [PubMed: 23742309]
13. Choi JM, Park WS, Song KY, Lee HJ, and Jung BH (2016) Development of simultaneous analysis of tryptophan metabolites in serum and gastric juice - an investigation towards establishing a biomarker test for gastric cancer diagnosis. Biomed. Chromatogr 30, 1963–1974. [PubMed: 27240299]
14. Henykova E, Vranova HP, Amakorova P, Pospisil T, Zukauskaite A, Vlckova M, Urbanek L, Novak O, Mares J, Kanovsky P, and Strnad M (2016) Stable isotope dilution ultra-high performance liquid chromatography-tandem mass spectrometry quantitative profiling of tryptophan-related neuroactive substances in human serum and cerebrospinal fluid, J. Chromatogr. A 1437, 145–157. [PubMed: 26879452]
15. Chen GY, Zhong W, Zhou Z, and Zhang Q (2018) Simultaneous determination of tryptophan and its 31 catabolites in mouse tissues by polarity switching UHPLC-SRM-MS. Anal. Chim. Acta 1037, 200–210. [PubMed: 30292294]
16. Hanstock CC, Rothman DL, Prichard JW, Jue T, and Shulman RG (1988) Spatially localized 1H NMR spectra of metabolites in the human brain. Proc. Natl. Acad. Sci. U. S. A 85, 1821–1825. [PubMed: 3162309]
17. Shulman RG and Rothman DL (2004) Metabolomics by In Vivo NMR, John Wiley & Sons, Ltd.
18. Shulman RG and Rothman DL (2001) 13C NMR of intermediary metabolism: implications for systemic physiology. Annu. Rev. Physiol 63, 15–48. [PubMed: 11181947]
19. Schroeder MA, Clarke K, Neubauer S, and Tyler DJ (2011) Hyperpolarized magnetic resonance: a novel technique for the in vivo assessment of cardiovascular disease. Circulation 124, 1580–1594. [PubMed: 21969318]
20. Richard DM, Dawes MA, Mathias CW, Acheson A, Hill-Kapturczak N, and Dougherty DM (2009) L-Tryptophan: basic metabolic functions, behavioral research and therapeutic indications. Int. J. Tryptophan Res 23, 45–60.
21. Ulrich AS (2005) Solid state 19F NMR methods for studying biomembranes. Prog. Nucl. Magn. Reson. Spectrosc 46, 1–21.
22. Patani GA and LaVoie EJ (1996) Bioisosterism: a rational approach in drug design. Chem. Rev 96, 3147–3176. [PubMed: 11848856]
23. Meanwell NA (2018) Fluorine and fluorinated motifs in the design and application of bioisosteres for drug design. J. Med. Chem 61, 5822–5880. [PubMed: 29400967]
24. Pan Y (2019) The dark side of fluorine. ACS Med. Chem. Lett, 10, 1016–1019. [PubMed: 31312400]
25. Rautio J, Gynther M, and Laine K (2013) LAT1-mediated prodrug uptake: a way to breach the blood-brain barrier? Ther. Deliv 4, 281–284. [PubMed: 23442072]

26. Jung MJ (1986) Substrates and inhibitors of aromatic amino acid decarboxylase. Bioorg. Chem 14, 429–443.
27. Leeds JM, Brown PJ, McGeehan GM, Brown FK, and Wiseman JS (1993) Isotope effects and alternative substrate reactivities for tryptophan 2,3-dioxygenase. J. Biol. Chem 268, 17781–17786. [PubMed: 8349662]
28. Chanut E, Trouvin JH, Bondoux D, Gardier A, Launay JM, and Jacquot C (1993) Metabolism of 6-fluoro-DL-tryptophan and its specific effects on the rat brain serotoninergic pathway. Biochem. Pharmacol 45, 1049–1057. [PubMed: 7681671]
29. Hoeltzli SD, and Frieden C (1995) Stopped-flow NMR spectroscopy: real-time unfolding studies of 6–19F-tryptophan-labeled Escherichia coli dihydrofolate reductase. Proc. Natl. Acad. Sci. U S A, 92, 9318–9322. [PubMed: 7568125]
30. Miwa S, Fujiwara M, Lee K, and Fujiwara M (1987) Determination of serotonin turnover in the rat brain using 6-fluorotryptophan. J. Neurochem, 48, 1577–1580. [PubMed: 2435850]
31. Rosenau CP, Jelier BJ, Gossert AD, and Togni A (2018) Exposing the origins of irreproducibility in fluorine NMR spectroscopy. Angew. Chem. Int. Ed. Engl 57, 9528–9533. [PubMed: 29663671]
32. Burden DW (2008) Guide to the homogenization of biological samples. Random Primers 7, 1–14.
33. Mu C, Yang Y, and Zhu W (2016) Gut microbiota: the brain peacekeeper. Front. Microbiol 7, 1–11. [PubMed: 26834723]
34. Dinan TG and Cryan JF (2017) Gut-brain axis in 2016: brain-gut-microbiota axis - mood, metabolism and behavior. Nat. Rev. Gastroenterol. Hepatol 14, 69–70. [PubMed: 28053341]
35. Collins SM, Surette M, and Bercik P (2012) The interplay between the intestinal microbiota and the brain. Nat. Rev. Microbiol 10, 735–742. [PubMed: 23000955]
36. Cryan JF and Dinan TG (2012) Mind-altering microorganisms: the impact of the gut microbiota on brain and behavior. Nat. Rev. Neurosci 13, 701–712. [PubMed: 22968153]
37. Keszthelyi D, Troost FJ, and Masclee AA (2009) Understanding the role of tryptophan and serotonin metabolism in gastrointestinal function. Neurogastroenterol. Motil 21, 1239–1249. [PubMed: 19650771]
38. Agus A, Planchais J, and Sokol H (2018) Gut microbiota regulation of tryptophan metabolism in health and disease. Cell Host Microbe. 23, 716–724. [PubMed: 29902437]
39. O'Mahony SM, Clarke G, Borre YE, Dinan TG, and Cryan JF (2015) Serotonin, tryptophan metabolism and the brain-gut-microbiome axis. Behav. Brain Res 277, 32–48. [PubMed: 25078296]
40. Francino MP (2016) Antibiotics and the human gut microbiome: dysbioses and accumulation of resistances. Front. Microbiol 6, 1–11.
41. Sternberg U, Klipfel M, Grage SL, Witter R, and Ulrich AS (2009) Calculation of fluorine chemical shift tensors for the interpretation of oriented 19F-NMR spectra of gramicidin A in membranes. Phys. Chem. Chem. Phys 11, 7048–7060. [PubMed: 19652840]
42. Becke AD (1993) A new mixing of Hartree–Fock and local density-functional theories. J. Chem. Phys 98, 1372–1377.
43. Becke AD (1993) Density-functional thermochemistry. III. The role of exact exchange. J. Chem. Phys 98, 5648–5652.
44. Lee C, Yang W, and Parr RG (1988) Development of the Colle-Salvetti correlation-energy formula into a functional of the electron density. Phys. Rev. B 37, 785–789.
45. Stephens PJ, Devlin FJ, Chabalowski CF, and Frisch MJ (1994) Ab Initio calculation of vibrational absorption and circular dichroism spectra using density functional force fields. J. Phys. Chem 98, 11623–11627.
46. Tirado-Rives J and Jorgensen WL (2008) Performance of B3LYP density functional methods for a large set of organic molecules. J. Chem. Theory Comput 4, 297–306. [PubMed: 26620661]
47. Wolinski K, Hinton JF, and Pulay P (1990) Efficient implementation of the gauge-independent atomic orbital method for NMR chemical shift calculations. J. Am. Chem. Soc 112, 8251–8260.
48. Marenich AV, Cramer CJ, and Truhlar DG (2009) Universal solvation model based on solute electron density and on a continuum model of the solvent defined by the bulk dielectric constant and atomic surface tensions. J. Phys. Chem. B 113, 6378–6396. [PubMed: 19366259]

49. Spartan'10 (Wavefunction, Ind.: Irvine, CA, USA (2010).

50. Gaussian 09, Revision B. 01 (Gaussian, Inc.: Wallingford, CT, USA, 2010).

51. Saunders CM, Khaled MB, Weaver JD III, and Tantillo DJ (2018) Prediction of 19F NMR chemical shifts for fluorinated aromatic compounds. J. Org. Chem 83, 3220–3225. [PubMed: 29470063]

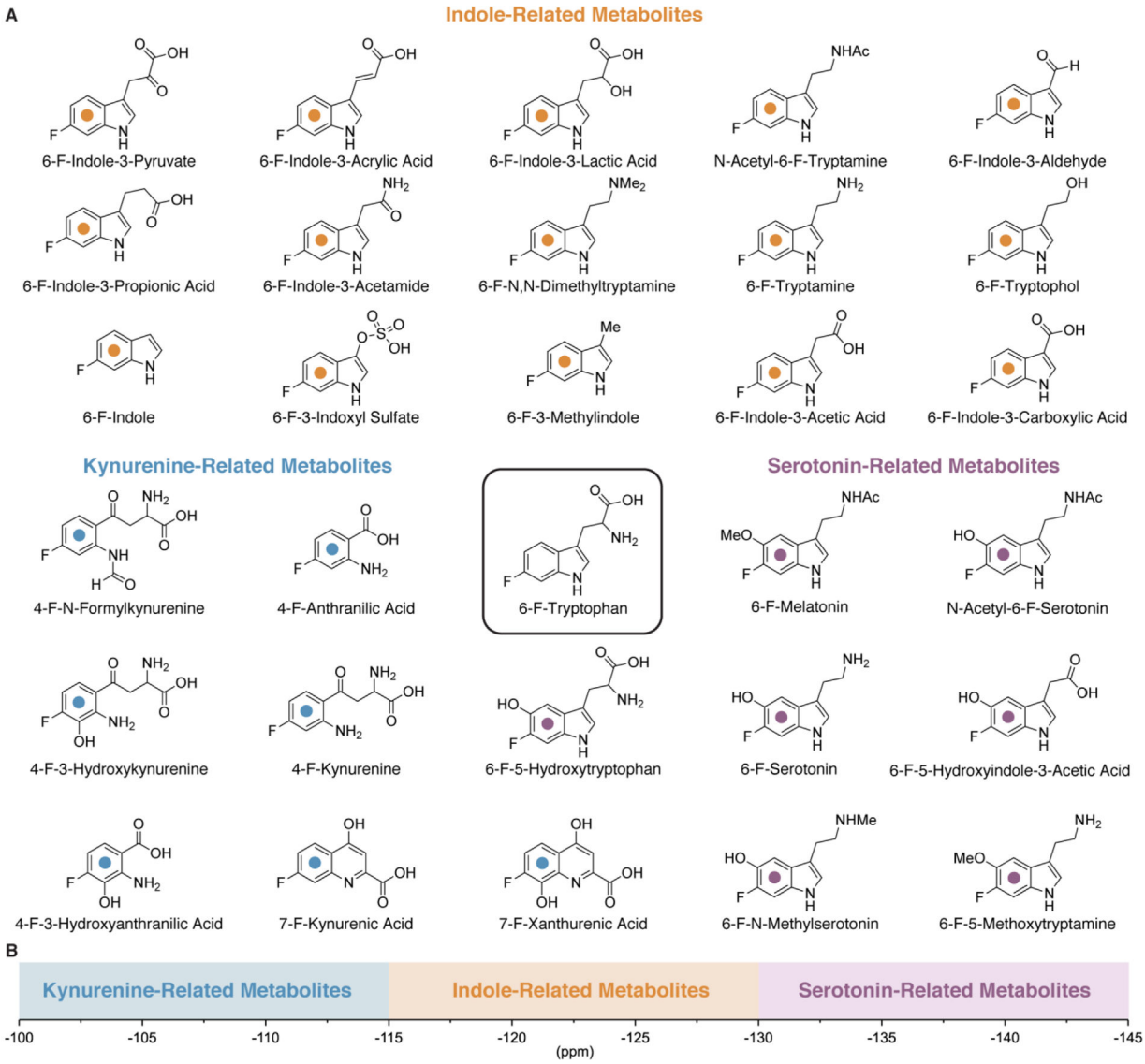

Figure 1.

A fluorinated probe for measuring tryptophan metabolism with ^{19}F nuclear magnetic resonance (NMR). (A) Possible metabolites of 6-F-tryptophan (6-F-Trp) categorized into three major metabolic pathways. (B) Approximate ^{19}F chemical shifts for metabolites from each of the three major tryptophan metabolic pathways.

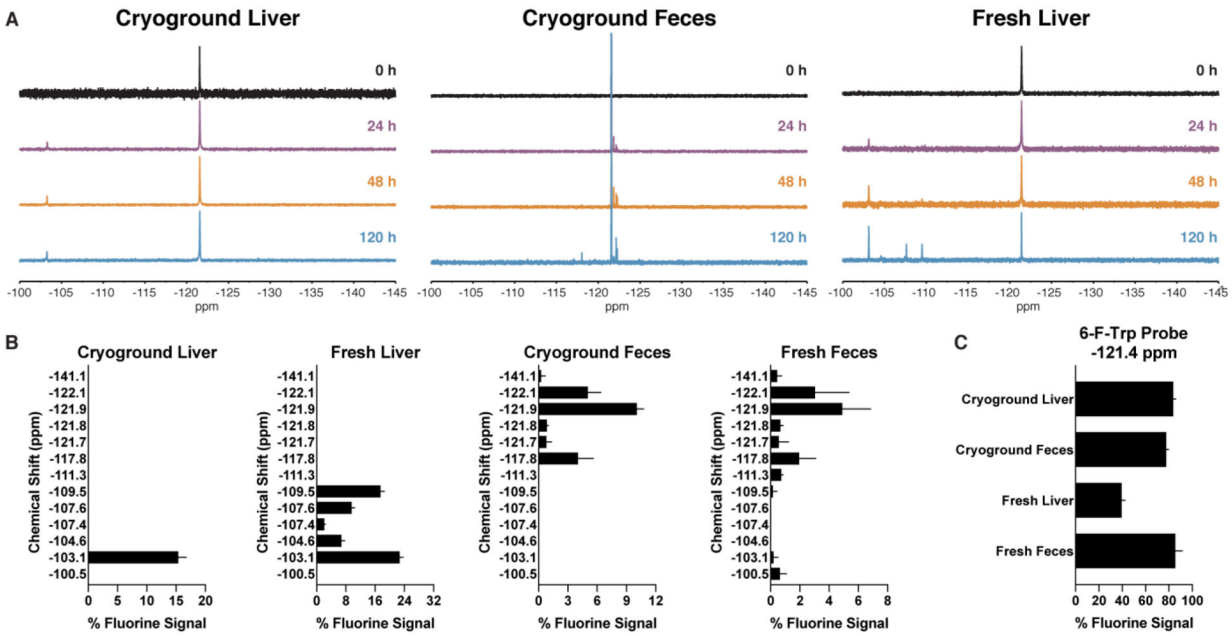

Figure 2.

Different tissues yield distinct metabolic profiles of 6-F-Trp. (A) Representative examples of fluorinated metabolites increasing as a function of incubation time in liver and fecal samples. (B) Metabolites with characteristic chemical shifts were measured after a 120 h ex vivo incubation period. The abundance of each metabolite is reported as a percent of the total fluorine signal obtained for that sample. (C) A reduction in ^{19}F NMR signal from 6-F-Trp (chemical shift = −121.4 ppm) was observed after a 120 h ex vivo incubation period for all tissues analyzed, with fresh liver yielding the most drastic reduction in probe concentration.

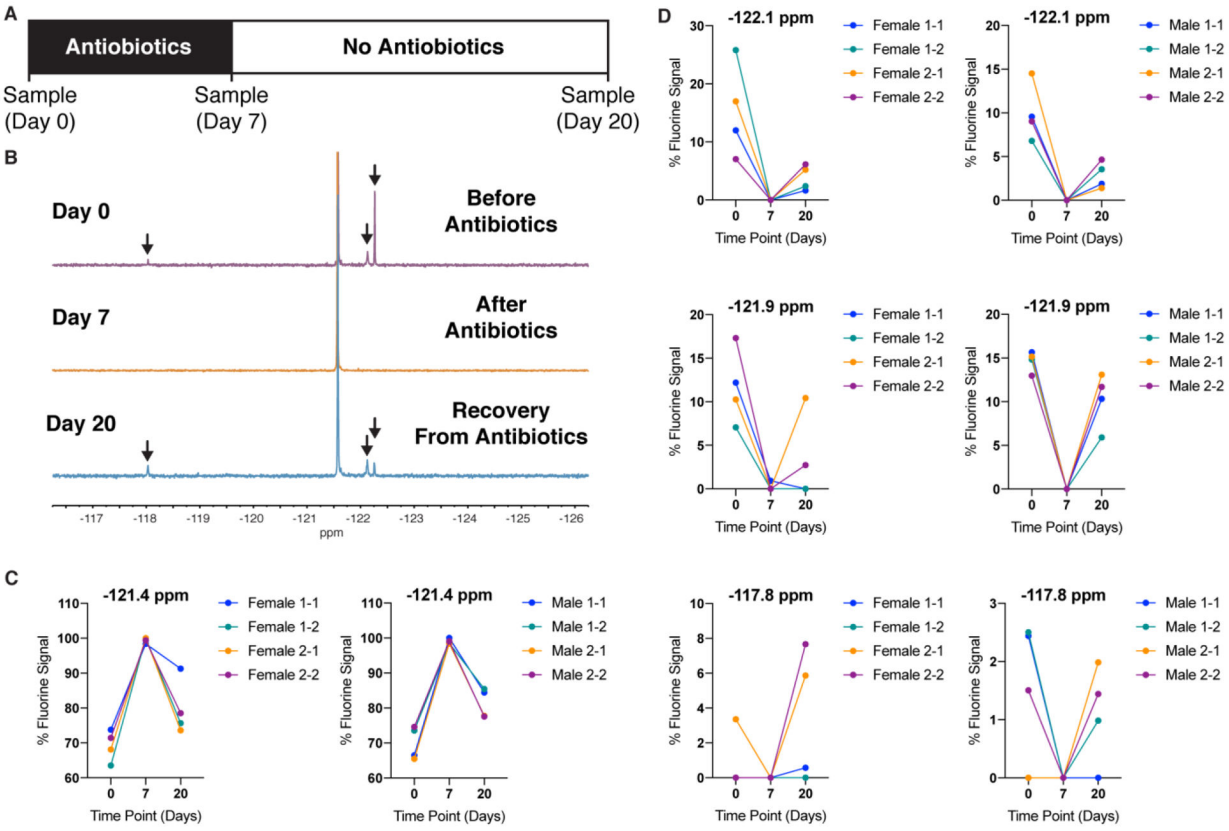

Figure 3.

Antibiotics disrupt tryptophan metabolism in the gut. (A) Experimental design. Fecal samples were collected before (Day 0), immediately after (Day 7), and 13 days after (Day 20) antibiotic administration. They were then incubated ex vivo with 6-F-Trp for 120 h before analysis. (B) Representative ^{19}F NMR spectra demonstrating that tryptophan metabolism is drastically reduced after antibiotic administration (Day 7) and does not fully recover even after nearly 2 weeks of cessation (Day 20). (C) Metabolism of 6-F-Trp (chemical shift = −121.4 ppm) is nearly abolished following one week of antibiotic treatment (Day 7). The extent of probe metabolism two weeks after cessation (Day 20) of antibiotics does not reach pre-antibiotic levels. (D) The effects of antibiotics on three of the most abundant 6-F-Trp metabolites are shown. Levels of each metabolite are expressed as percentages of the total fluorine signal obtained for that sample. See Figure S3 for quantification of other metabolites. The sex, cage number, and animal number (e.g., Female 1–1 = female, cage 1, animal 1) are indicated.

Table 1.

Calculated ^{19}F NMR Chemical Shifts for 6-F-Trp Metabolites

Compound	Calculated Shift (ppm)	Experimental Shift (ppm)	Deviation[a] (ppm)	Pathway
6-F-N-Formylkynurenine	−93.10	–	–	Kynurenine
6-F-Kynurenine	−97.84	–	–	Kynurenine
6-F-Kynurenic Acid	−101.08	–	–	Kynurenine
4-F-Anthranilic Acid	−106.75	−107.3	0.55	Kynurenine
3-F-Aniline	−112.17	−113.3	1.13	Control[b]
6-F-Indole-3-Aldehyde	−116.41	–	–	Bacteria
6-F-Indole-3-Acrylic Acid	−118.50	–	–	Bacteria
6-F-3-Indoxyl Sulfate	−119.76	–	–	Bacteria
6-F-Indole-3-Carboxylic Acid	−119.89	–	–	Bacteria
6-F-Indole-3-Pyruvate	−121.02	–	–	Bacteria
6-F-Indole-3-Acetic Acid	−121.65	–	–	Bacteria
6-F-Indole	−121.74	–	–	Bacteria
6-F-Indole-3-Lactic Acid	−121.88	–	–	Bacteria
6-F-Indole-3-Propionic Acid	−122.19	–	–	Bacteria
6-F-Tryptophan	−122.52	−121.4	−1.12	Bacteria
6-F-N,N-Dimethyltryptamine	−122.52	−121.3	−1.22	Bacteria
6-F-Indole-3-Acetamide	−122.60	–	–	Bacteria
N-Acetyl-6-F-Tryptamine	−122.68	–	–	Bacteria
6-F-3-Methylindole	−122.82	–	–	Bacteria
6-F-Tryptamine	−122.98	−121.4	−1.58	Bacteria
6-F-Tryptophol	−123.13	–	–	Bacteria
4-F-3-Hydroxykynurenine	−129.17	–	–	Kynurenine
6-F-5-Methoxytryptamine	−133.19	–	–	Serotonin
4-F-3-Hydroxyanthranilic Acid	−133.80	–	–	Kynurenine
7-F-Xanthurenic Acid	−135.71	–	–	Kynurenine
6-F-Melatonin	−139.91	–	–	Serotonin
4-Amino-2-F-Phenol	−140.04	−139.3	−0.74	Control[b]
6-F-5-Hydroxyindole-3-Acetic Acid	−147.00	–	–	Serotonin
6-F-5-Hydroxytryptophan	−147.90	–	–	Serotonin
6-F-Serotonin	−148.44	–	–	Serotonin
6-F-N-Methylserotonin	−148.51	–	–	Serotonin
N-Acetyl-6-F-Serotonin	−149.26	–	–	Serotonin

[a]Deviation = Calculated – Experimental.

[b]Control compounds used to validate our calculations. The remainder of the compounds in the table represent expected metabolites of 6-F-Trp. – = data not available